XIII ICSMFE, 1994, New Delhi, India / XIII CIMSTF, 1994, New Delhi, Inde

MEASURED PRESSURES AND STRAINS IN SILOS STORING GRANULAR MATERIALS

MEASURES DE PRESSIONS ET TENSIONS EN SILOS DE STOCKAGE POUR MATERIAUX GRANULAIRES

Geoffrey E. Blight

Professor of Construction Materials
Witwatersrand University, Johannesburg, South Africa

SYNOPSIS: A program to measure silo pressures and frictional wall loads in full size silos storing granular materials has been conducted over the past 17 years. The paper summarizes some of the more recent findings of the work. These include observations of the nature of pressures and strains in silos during filling and the changes that occur at the start of emptying. Pressures and strains for silos may be non-uniform around the perimeter and are dependent on thermal effects.

INTRODUCTION

Since 1973 the writer has conducted a program to measure silo pressures and frictional wall loads in full-size silos storing granular materials and powders. The objective has been to examine the validity of generally accepted design assumptions, as incorporated into current silo design codes and procedures. The program has made a detailed investigation of pressures and wall loads in 20 storage structures with diameters ranging from 5.5m to 25m and capacities from 250 tons to 15 000 tons. Lesser investigations have been carried out on 4 other silos. Materials stored have ranged from coal and cement powder to mineral ores, granulated sugar and grain of various types. The range of structures has included reinforced concrete bins and silos, plane plate welded steel silos and stiffened bolted corrugated steel silos. Pressures have been measured directly by means of calibrated pressure cells, and wall loads and pressures have also been inferred via electric resistance strain gauge measurements.

PRESSURE-DEPTH PROFILES DURING FILLING AND AT START OF EMPTYING OF CYLINDRICAL SILOS

Most accepted design codes and guidelines for estimating lateral pressures on silo walls, eg. Deutsches Institut Für Normung (DIN) (1987), Institution of Engineers (Australia) (1986), recognise that there may be an increase in lateral pressure when emptying of a full silo is started. Most codes and guidelines also recommend the use of the Janssen equation for estimating lateral pressures. The process whereby the increase of pressure occurs is not well understood. Explanations vary from a break-down of Janssen-type arching [eg. Reynolds (1932)] to the generation of a transient over-pressure or switch pressure as the stress state of the silo contents changes from an "active" to a "passive" state [Jenike (1964)]. In addition most design codes consider two load conditions, those of "end of filling" and "start of emptying", as being the critical cases for design. It is these two conditions that will be concentrated on in this paper, together with a third condition, that which applies when a full silo is subjected to daily temperature cycles with its contents static. Some design codes distinguish between pressures suitable for mass flow silos and funnel flow silos. All of the silos dealt with in this paper are funnel flow silos, but it actually makes little or no difference which flow regime applies.

Figure 1 shows the results of pressure measurements on a 20m diameter coal storage and load-out silo. The silo has a slot outlet 2m wide by 7m long and the base is benched at fairly flat angles varying from 50° to 57° so that the coal will not slide on and abrade the benching. The pressures were measured by means of pressure cells of the mercury-filled strain-gauged diaphragm type and were calibrated using coal before installation. All of the pressure cells for which measurements are shown in Figure 1 were installed on the vertical cylindrical walls of the silo, although gauges were also installed lower down on the benching.

Figure 2 shows the results of laboratory compression tests on samples of coal taken at different times from the belt feeding the silo. Triaxial shear tests established the active pressure coefficient K_A at between 0.21 and 0.23 while triaxial compression tests with zero lateral strain showed that the at rest pressure coefficient Ko varied with the moisture content of the coal, but lay between 0.44 and 0.67. It will be noted that the relationship between σ_1 and σ_3 is not linear, but approaches linearity.

The pressure profiles shown in Figure 1 were measured at various stages during filling of the silo, and at the start of emptying. They show that the relationship between depth of coal above a certain point and pressure is approximately linear and that the form of the relationship remains more or less constant as the silo is filled. At the start of emptying, certain of the pressures increased while others decreased.

Figure 3 shows the pressures plotted in a similar format to that of Figure 2. The calculated overburden stress γz replaces σ_1 and the measured horizontal pressure σ_h replaces σ_3. The similarity between Figures 2 and 3 is obvious, but there are differences. During filling, measured pressures clustered about the lines labelled K_A with some pressures approaching the Ko lines. This indicates mainly an active state of stress, ie. a state of failure, with σ_h less than σ_v in the coal during filling. As the material falls into the silo, it lands,

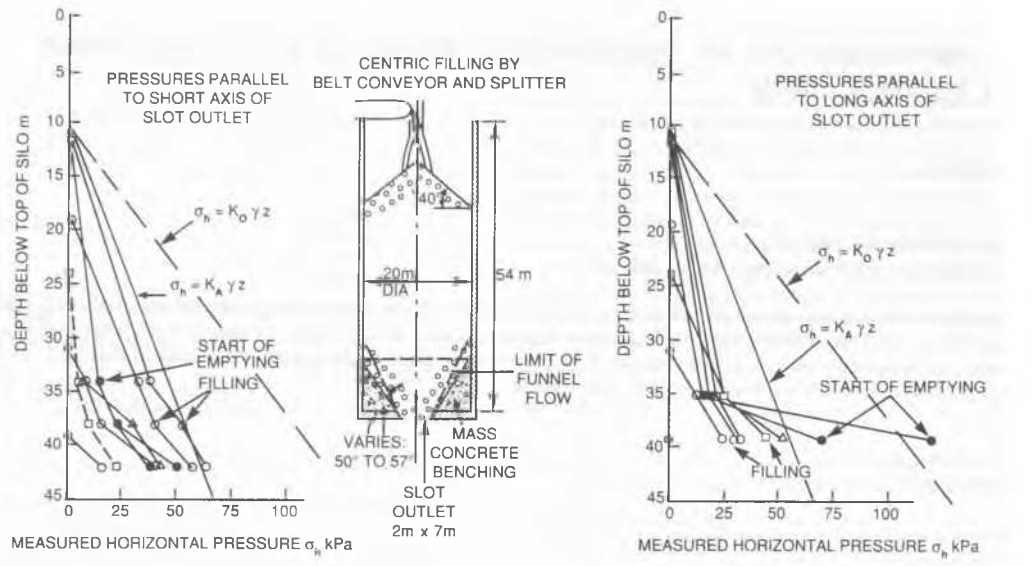

FIGURE 1: Profiles of horizontal pressure measured in reinforced concrete coal load-out silo during filling and at start of emptying.

rolls and slides on the slopes of a cone of deposition. It is thus deposited in a state of failure and in this case appears to remain in this state as the overburden builds up over it.

It will be seen from Figure 1 that all of the pressures parallel to the short axis of the outlet (i.e. across the slot) decreased, while the pressures that increased were those directed along the slot. Figure 3 shows that the decreased pressures correspond to an apparent K value of 0.15. However, K_A is the lowest pressure ratio that theoretically can apply in a granular material. The only obvious explanation for these low pressures is that σ_v also decreased at the start of emptying with the decrease induced by Janssen-type

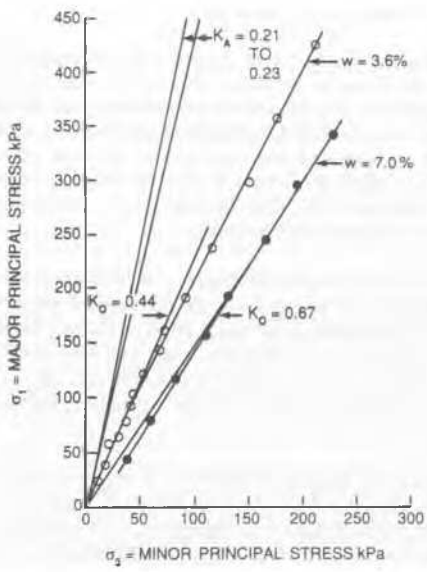

FIGURE 2: Relationship between major and minor principal stresses during compression of coal under at-rest (K_o) and active (K_A) conditions.

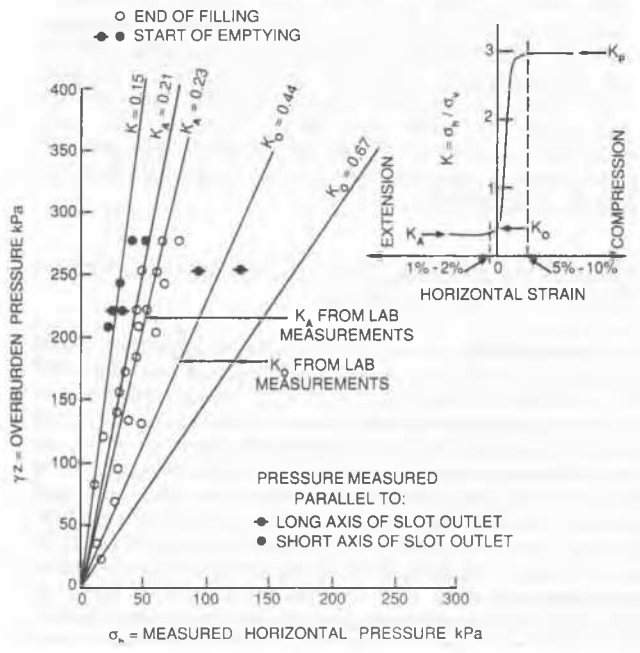

FIGURE 3: Relationship between overburden pressure and measured horizontal pressure for silo referred to by Figure 1 during filling and at start of emptying.

arching across the slot. Along the slot, one pressure cell showed a marked increase in pressure, with the pressures moving towards the Ko state, while the other showed no change. It appears that the changes of pressure that occur at the start of emptying are very complex and are related to the geometry of the outlet. Depending on circumstances, pressures may either increase or decrease.

The pressure cells used to produce Figure 1 were all located in the zone within which the flow funnel to the outlet would have been expected to intersect the cylindrical walls of the silo. When the silo was emptied, a flow funnel or equivalent hopper surface of compacted coal remained in place, showing that the flow funnel actually intersected the silo wall at a depth of 37m below the top of the silo. According to the "switch" or "peak" pressure theories of Jenike (1964) and Walker (1966), it is in this zone that an increased or switch pressure will develop at the start of emptying. An important part of the argument for the existence of switch pressures is that the silo filling is forced to compress as it flows towards the silo outlet and therefore the pressure coefficient switches from K_A (with values in the region of 0.2 to 0.3) to K_p, the passive pressure coefficient (with values of 3 to 5).

The inset on Figure 3, which appears in most standard texts on earth pressure, shows that the switch from K_A to K_p cannot occur without a considerable lateral compression of the silo filling. This would only take place if the filling were squeezed into the conical space of the hopper. On the other hand, studies of flow patterns at the exit of silos [eg. Deutsch and Clyde (1967)] appear to show that the filling is not squeezed into the outlet, but "queues" to exit. If this is what happens, there is no reason for a sudden change of pressure coefficient at the start of emptying, and hence no reason for a switch pressure. The queuing action, would however not be inconsistent with the moderate changes in pressure demonstrated in Figure 1.

Figure 4 presents the results of strain measurements on the 5.5m diameter bolted corrugated steel wheat silo shown in the centre of the diagram. The measurements to the left were taken on the same vertical line at the levels shown in the central diagram. The hoop strains have been expressed as inferred lateral pressures and are plotted against the corresponding overburden pressures. To emphasise that these measurements are interpreted strains, and not directly measured pressures, the symbol p_h will be used to denote lateral pressures inferred from the strains. The measurements represent a series of inferred pressure paths for the points of measurement showing how the pressure increases as filling proceeds and is followed by the start of emptying.

It will be seen that the inferred lateral pressure at each of the points 0, 1, 2 increased progressively until the silo was full. At the start of emptying there was a further increase of inferred pressure, as indicated by the arrows. In each case the pressure approached the $K_A\gamma z$ line or active state line.

The set of measurements on the right is similar, except that all measurements were taken at the same level, but spaced at 120° intervals in plan around the perimeter of the silo. Similar behaviour is evident at the start of emptying for this set of data.

The fact that inferred pressures were less than those for the $K_A\gamma z$ line during filling indicates that Janssen type arching was occurring during filling. The increase in pressure at the start of emptying would, in terms of the Janssen theory, indicate that the arching was reduced, vertical pressures increased and the material approached a no-arching active state.

In the case of the measurements on the left of Figure 4, a continuous chart recording was made of the variation of strain with time after the start of emptying. The recording is shown in Figure 5 where the strains have also been expressed as inferred lateral pressures. At all three points, strains gradually increased to the end values shown in Figure 4. The points of measurement were deliberately placed in positions adjacent to where the flow cone would be expected to intersect the wall, and where transient or static switch pressures would be expected to occur. The behaviour shown in Figure 5, also does not seem consistent with the generation of a switch pressure. The moderate increases in pressure are, however, consistent with a loss of arching. In the two cases examined here, the silo with a slot outlet showed decreases of lateral pressure across the slot, where arching is most likely to occur

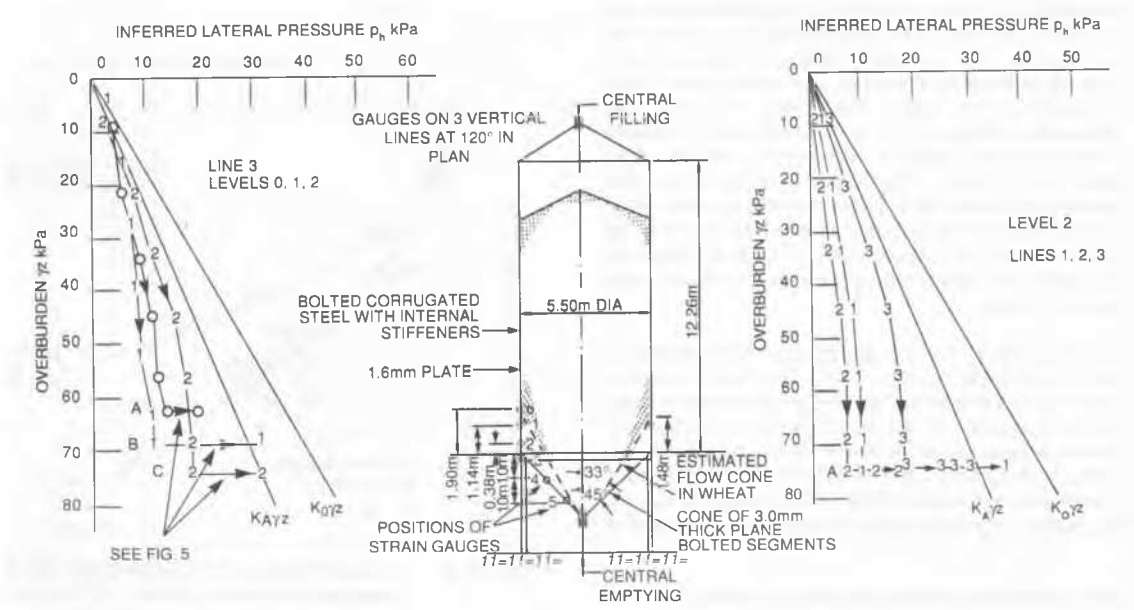

FIGURE 4: Stress paths for inferred lateral pressures in cylindrical portion of stiffened corrugated-steel silo during filling with wheat and at start of emptying.

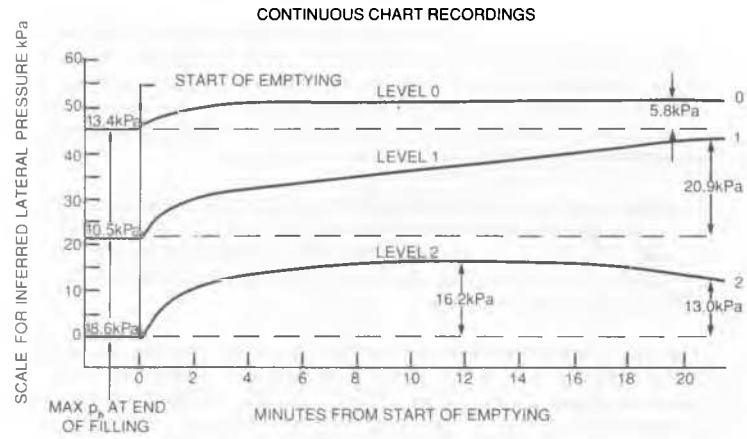

FIGURE 5: Continuous recordings of strain expressed as equivalent lateral pressure, with time after start of emptying for silo referred to by Figure 4.

at the start of emptying, and increases of pressure along the slot. In the second case, where the outlet is symmetrical, only increases in pressure, consistent with a loss of arching, were recorded. A number of cases where changes of pressure at the start of emptying show similar characteristics have been described by Blight (1990).

Figure 6 shows a set of inferred lateral pressures measured during filling of a silo identical to that illustrated in Figure 4 except that the barrel is supported on the ground and there is no conical hopper. The material being stored was barley. In this set of data, strains were measured both on the inside and on the outside of the corrugated steel silo wall, at two different heights and at four positions around the perimeter. Differences between comparative measurements were found to be within the scatter of measurements made on the outside. Most of the measurements follow the Janssen pressure line labelled "arching $K=K_A$", calculated for a lateral pressure coefficient of K_A. However, a significant number of measurements indicate that the lateral pressure over part of the perimeter of the silo lies on the line given by $p_h = K_o\gamma z$ where Ko, the at rest pressure coefficient was established by laboratory tests like those shown in Figure 2. The lower part of Figure 7 shows strain measurements on the stiffeners of the silo, interpreted as stiffener loads. The measurements agree reasonably well with the relationship between stiffener load and overburden pressure calculated by the Janssen equation with $K=K_A$ and the fully developed angle of wall friction.. The measurements are less than what would be expected for a linear stress distribution with depth and a pressure coefficient of Ko unless it is assumed that the full angle of wall friction was not developed. The observations of stiffener load are, however, reasonably consistent with the inferred lateral pressures in the silo.

The data shown in Figures 1, 4 and 6 are typical of lateral pressure profiles recorded in a number of other silos. The data show that Janssen-type arching may or may not occur in silos during filling and that the stress state adjacent to the wall may correspond to any state from Janssen arching active, to active, to a rest (Ko). At the start of emptying, pressures in the area where the flow cone intersects the wall may decrease or increase, depending on the geometry of the outlet. However, switch pressure do not seem to occur.

TEMPERATURE SURCHARGE PRESSURES IN SILO WALLS

Temperature surcharge pressures arise when the wall of a silo contracts in response to a diurnal or seasonal fall in temperature (see Figure 7). The contraction is resisted by the silo filling with the result that the silo wall experiences an increase in pressure. When the wall expands again, the pressure reduces. However, a residual pressure remains because the silo fill moves progressively outwards with the wall as it expands, and then increases the restraint offered to contraction of the wall when it cools again. The result is a thermal ratcheting effect in which the pressure in the silo builds up to a maximum over a period of 3 to 5 days. The ratcheting action has been demonstrated by Blight (1985). This additional pressure has been called the temperature surcharge pressure. The thermal effect is shown in Figure 8 for a 24m diameter reinforced concrete silo storing cement powder. In this diagram the horizontal pressure on the wall was measured by a mercury filled strain-gauged diaphragm pressure cell set in the silo wall. The effect is even more marked for steel silos where the walls respond more quickly to changes in ambient temperature [eg. Blight (1985)].

The temperature surcharge pressure appears first to have been investigated by Anderson (1966). However, his expression for the temperature surcharge pressure is hard to use realistically because of the difficulty of correctly evaluating the materials properties it incorporates. The method requires the evaluation of the elastic modulus and Poisson's ratio for the silo filling. Moduli for granular

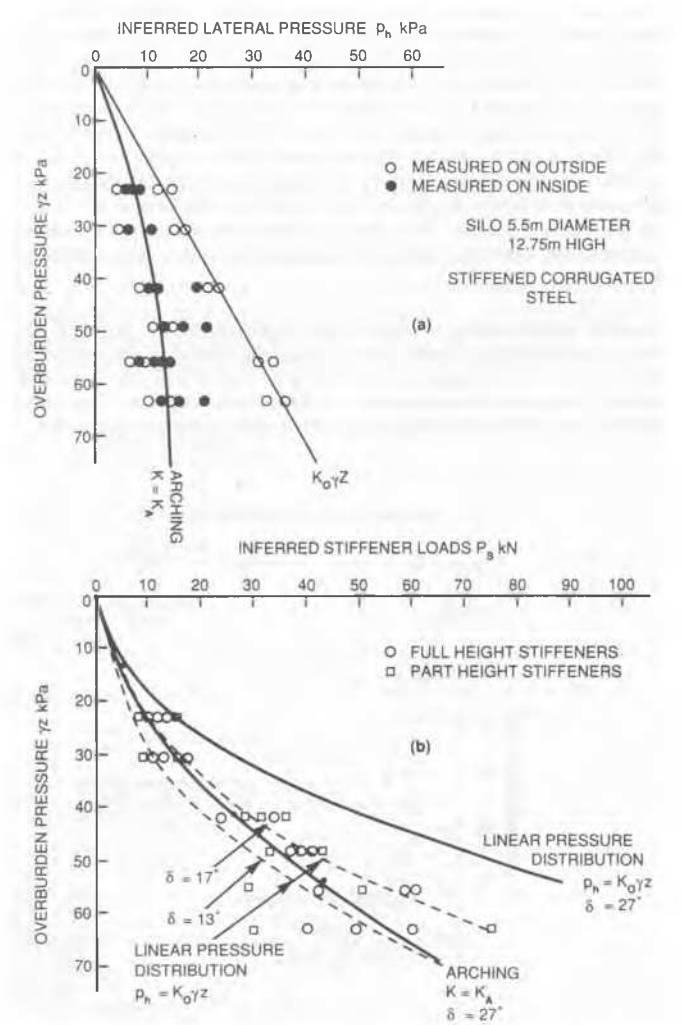

FIGURE 6: (Above) Stress path measurements for inferred lateral pressures for silo identical to that of Fig.4, but ground-supported and storing barley.
(Below) Load paths for inferred stiffener loads for same silo.

and powdered materials are highly sensitive to strain, and reduce rapidly with increasing strain. As temperature surcharge pressures develop at strains of 100 to 200 microstrain, it is necessary to measure the corresponding moduli at this strain level. Because it is difficult to take into account radial variations of strain, the author has developed an alternative equation [Blight (1990)] containing materials properties that can be inferred from measurements of thermal strain on prototype silos. The equation for the temperature surcharge TS is essentially the same as Anderson's, and is as follows for a (cylindrical silo):

$$TS = \frac{2M_s E t \varepsilon_f}{M_s D + 2Et} \qquad (1)$$

in which M_s is the modulus of compressibility of the silo filling for horizontal radial compression;

E is the modulus of elasticity for the material of the silo wall;

D is the mean diameter of the silo;

t is the wall thickness; and

ε_f is the mean free thermal strain in the wall, ie. the mean strain that would occur were the silo empty.

TS has been evaluated from strain and temperature or pressure and temperature recordings similar to those shown in Figures 7 and 8.

For the case illustrated in Figure 8, where the outside face of the wall changed temperature by $\Delta\theta_o$ and the inside by $\Delta\theta_i$.

$$\varepsilon_f = \frac{\alpha}{2}(\Delta\theta o + \Delta\theta_i) \qquad (2)$$

where α is the coefficient of thermal contraction of the wall.

Figure 9 assembles all the values of M_s that are currently available. Most of these have been deduced from measurements on steel grain silos. Fortunately the compression modulus M_s seems to be fairly similar for most grains. Even cement powder lies fairly close to the line of best fit to all of the observations. The modulus M_s is very difficult to measure with any accuracy, as the temperature of a silo is never uniform around its circumference, especially when the silo wall is partly in sun and partly in shade. The values of M_s shown in Figure 9 were made by recording thermal strain and the corresponding temperature over several 24 hour cycles in order to minimize the effect of the non-uniformity of temperature around the silo perimeter.

CONCLUSIONS

1. The data shown in Figures 1 and 6 show that it is difficult to know, at the design stage, if a Janssen-type lateral pressure distribution will occur in a silo. Such a distribution may occur only over part of the silo perimeter (Figure 6), or the arch action may disappear at the start of emptying (Figures 4 and 5). For design purposes it is safe and realistic to assume that the maximum pressure to which the silo wall will be subjected will be given by

$$p_h = K_o \gamma z$$

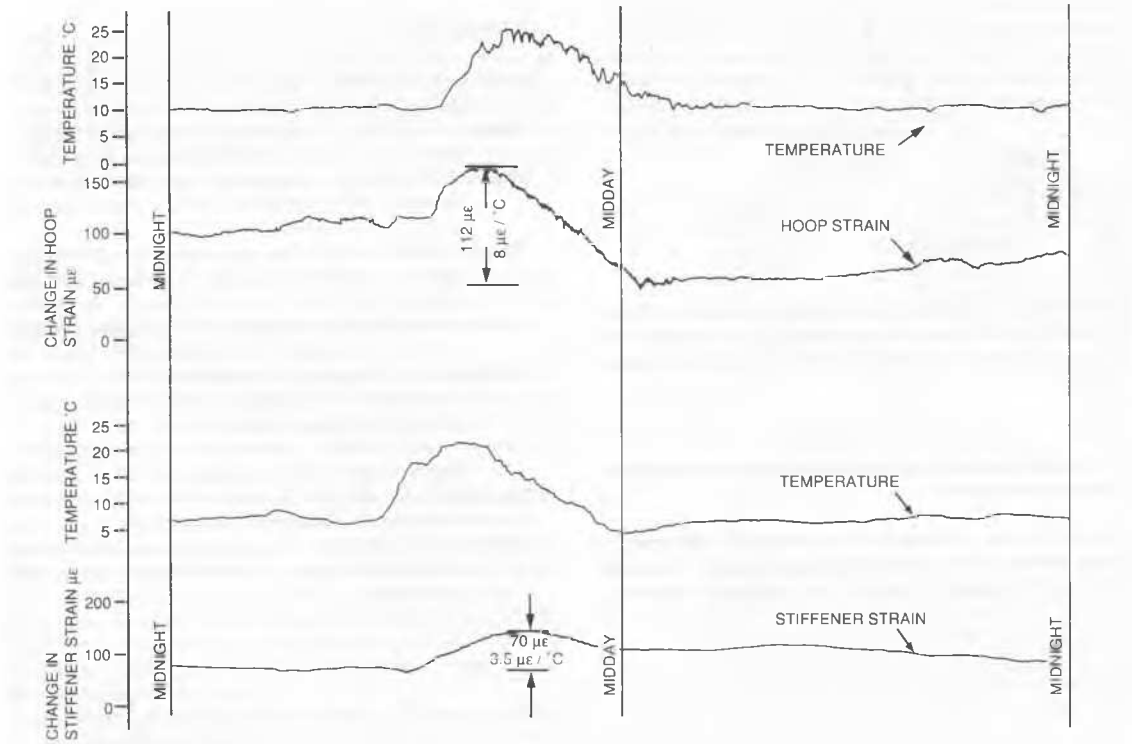

FIGURE 7: Variation over 24-hour period of temperature, hoop strain and stiffener strain for are of wall of corrugated-steel grain silo.

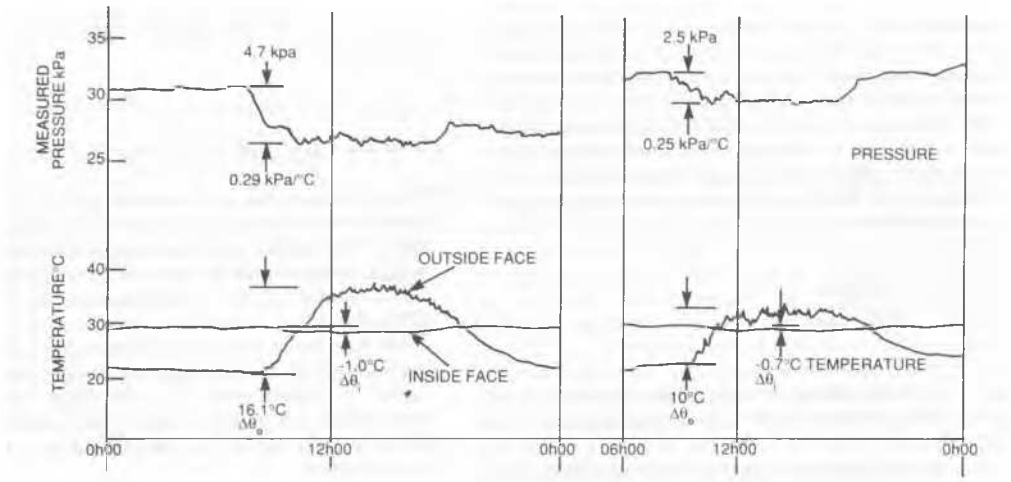

FIGURE 8: Variation over two daily periods of temperature and lateral pressure on the wall of a 24m diameter reinforced concrete silo storing cement powder.

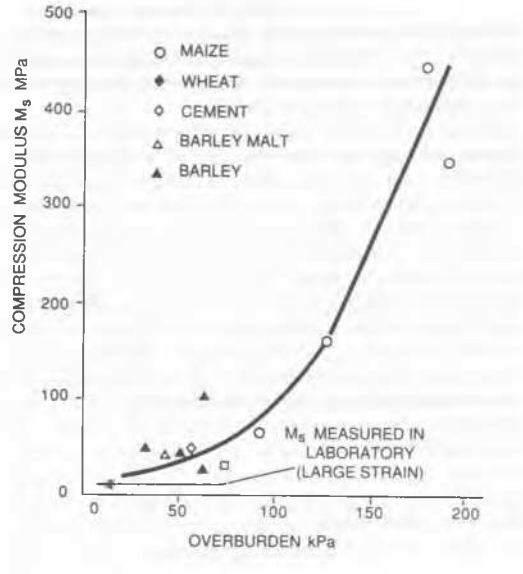

FIGURE 9: Relationship between compression modulus M_s and overburden stress calculated from measurements on 10 steel grain silos and reinforced concrete cement silo.

while recognizing that the pressure may not everywhere be given by this expression.

2. Silo pressures can be expected to change at the start of emptying, although the changes may be localized. Pressures may increase (Figures 1 and 4) or decrease (Figure 1) depending on the geometry of the outlet. Changes of pressure take place in a gradual fashion (Figure 5) and static or transient switch pressures do not seem to occur.

3. Silo pressures and frictional wall loads can vary considerably as a result of temperature changes. This applies to both reinforced concrete and steel silos (Figures 7 and 8).

4. Temperature surcharge pressures for a limited number of silo fillings can be predicted on the basis of equation (1) and values of the modulus M_s from Figure 9.

REFERENCES

Anderson, P. (1966). "Temperature stresses in steel grain storage tanks", Civil Engineering, ASCE, Jan, 74.

Blight, G.E. (1985). "Temperature changes affect pressures in steel bins", Int. J. Bulk Solids Storage in Silos (UK), 1 (3), 1-7.

Blight, G.E. (1990). "Defects in accepted methods of estimating design loading for silos". Proc. Instn. Civ. Engrs (U.K) Part 1, 88, 1015-1036.

Deutsch, G.P. and Clyde, D.H. (1967). "Flow and pressure in granular materials in silos." J. Engg Mech Div, ASCE 93 (EM6) 102-125.

Deutsches Institut für Normung (1987). "Lastannahmen für Bauten-Lasten in Silozellen", DIN, Berlin DIN 1055, Part 6.

Institution of Engineers, Australia (1986), "Guidelines for the assessment of loads on bulk solids containers". The Institution, Melbourne.

Jenike, A.W. (1964). "Storage and flow of solids." Engineering Experiment Station, University of Utah, Bulletin 123.

Reynolds, C.E. (1932). "Reinforced concrete designer's handbook." Concrete Publications, London, UK.

Walker, D.M. (1966). "An approximate theory for pressures and arching in hoppers." Chemical Engineering Science (UK) 21, 875-997).